

UNCLASSIFIED

Defense Technical Information Center  
Compilation Part Notice

ADP010918

TITLE: Fractal and Topological Complexity of  
Radioactive Contamination

DISTRIBUTION: Approved for public release, distribution unlimited

This paper is part of the following report:

TITLE: Paradigms of Complexity. Fractals and  
Structures in the Sciences

To order the complete compilation report, use: ADA392358

The component part is provided here to allow users access to individually authored sections of proceedings, annals, symposia, ect. However, the component should be considered within the context of the overall compilation report and not as a stand-alone technical report.

The following component part numbers comprise the compilation report:

ADP010895 thru ADP010929

UNCLASSIFIED

## FRactal and Topological Complexity of Radioactive Contamination

N. G. MAKARENKO, L. M. KARIMOVA

*Institute of Mathematics, 125 Pushkin str.,  
480100, Almaty, Kazakhstan  
E-mail: makarenk@math.kz*

A. G. TEREKHOV

*Institute of Space Research, 26 Shevchenko str.,  
480100, Almaty, Kazakhstan  
E-mail: remote@astel.kz*

M. M. NOVAK

*School of Physics, Kingston University,  
Surrey KT1 2EE, England  
E-mail: novak@kingston.ac.uk*

There is verified the hypothesis about multifractal nature of radioactive contamination due to nuclear explosions on Semipalatinsk test site (STS) in Kazakhstan. The fields of terrestrial contamination have extreme high variability caused by a number of nature processes. There are used the methods of multifractal formalism and computation topology. The results of analysis support the existence of multifractal scaling, which is different for natural and man-made isotopes. It means that there are "hot spots" of man-made *Cs* isotope contamination dangerous for human health, which can't be detected by the traditional in Kazakhstan technics of measurements from air. Moreover, the finding of self-similarity could be the base of new methods of diagnostics of large territories.

### 1 Introduction

There were some 470 nuclear explosions on STS in Kazakhstan, of which 90 explosions were in the air, 25 on the ground and 355 underground. As a result a lot of territories were contaminated and it has become a matter of serious for people with regard to its consequences for the lives and health<sup>1</sup>. We analyze the resulting contaminated areas by examining the distribution of radionuclides. The analysis of the problem is not trivial and is influenced by a number of issues, such as wide range of contamination, extending from meters to hundreds of kilometers; presence of a mixture of radioactive isotopes, due to numerous nuclear explosions of various composition and power; highly variable rate of migration of radionuclides in soils; the influence of climatic conditions on the localisation of contamination and its transport<sup>2</sup>. So, the radioactive contamination of the ground is a result from nonlinear interplay of geophysical fields which intervene over a large range of scale. Consequently, fields of contamination observed have an extreme spatial variability, frequently cited "hot spots" or "leopard's skin"<sup>3</sup>.

Complex structure of the field is the main difficulties of it's diagnostics. The absence of the field smoothness restricts a choice of methods of measurements and data processing. The maps of contamination are designed using interpolation of

measurements and, consequently, depend on a scale of averaging. As a result, sparse anomalies can be missed.

To detect all fluctuations of the contamination field measurements must cover a territory by a network of overlap neighborhoods<sup>4</sup>. But it is impossible for huge areas of former nuclear weapon testing site, spanning an area of around 18500km<sup>2</sup> and regions bordering this test site which we deal with. Nowadays, only 1% of contaminated territory has been investigated by accepted in Kazakhstan methods of measurements from air and it is definitely not enough to describe the radioactive contamination and to implement effective decontamination methods. The scale-symmetry assumption is the simplest and also only one acceptable in the absence of knowledge in specific mechanisms producing these fields. The idea of scaling invariance can be useful in practice and could become a base for the analysis and diagnostics of the areas.

The present study deals with the area-analysis of the distribution of radionuclides in Kazakhstan. The data is obtained primarily from former STS and, secondly, from regions bordering this test site. Experimental data consist of radionuclide measurements made from the air, on a grid of parallel lines covering a part of territory. Two regions, Karaganda and Semipalatinsk, and Irtysh test site were explored.

It is possible to analyze these measurements by several complementary methods, among them the fractal<sup>5</sup>, multifractal<sup>3,6</sup> and morphology methods<sup>7</sup>. Here, we present multifractal method<sup>8,9</sup> and method of computational topology<sup>10</sup>.

The structure of this paper is as follows. In Sec. 2 we recall some definitions of multifractal analysis and apply this technique to the data from flight paths. In Sec. 3 we describe the method of computational topology and present the results of applying this method and multifractal one to data from the Irtysh test site. The summary is found in the concluding section.

## 2 Multifractal analysis of radioactive contamination

We used an approach in which the contamination data along a path are considered as multifractal random measures. Let us remind<sup>8,9,11</sup>, that multifractal spectrum of singularities  $\alpha$  of Borel finite measure  $\mu$  on a \*compact\* set  $X$  is a function  $f(\alpha)$  defined by pair  $(g, G)$ . Here,  $g : X \rightarrow [-\infty, \infty]$  is a function, which determines the level sets:

$$K_\alpha^g = \{x \in X : g(x) = \alpha\} \quad (1)$$

and produces a multifractal decomposition  $X$ :

$$X = \bigcup_{-\infty \leq \alpha \leq \infty} K_\alpha^g. \quad (2)$$

Let  $G$  be a real function which is defined on  $Z_i \subset X$  such as  $G(Z_1) \leq G(Z_2)$  if  $Z_1 \subset Z_2$ . Then multifractal spectrum is  $f(\alpha) = G(K_\alpha^g)$ . Let  $g$  be determined as pointwise dimension  $d_\mu$  of measure  $\mu(x)$  at all points  $x \in X$  for which the limit

$$g \equiv d_\mu(x) = \lim_{r \rightarrow 0} \log \mu(B(x, r)) / \log r, \quad (3)$$

exists, where  $\mu(B(x, r))$  is a "mass" of measure in the ball of radius  $r$  centered at  $x$ . Since, we have chosen  $g = d_\mu$ , we can drop the  $g$  subscript from further references to  $K_\alpha^g$ . Then  $K_\alpha = \{x : d_\mu(x) = \alpha\}$ , where exponent  $\alpha$  is local density of  $\mu$ . The singular distribution  $\mu$  can then be characterized by giving the "size" of sets  $K_\alpha$  by their Hausdorff dimension, i.e.  $f(\alpha) = G(K_\alpha) = \dim_H(K_\alpha)$ . If  $\mu$  is self-similar in some sense,  $f(\alpha)$  is a well behaved concave function of  $\alpha$ <sup>9</sup>. To estimate  $f(\alpha)$  for path data we applied the method of the partition sum<sup>11</sup>.

Let  $X = \mathfrak{S} = [0, 1]$  and  $k_n$  be an increasing sequence of positive integers. Define:

$$I_{i,n} = \left[ \frac{i}{k_n}, \frac{i+1}{k_n} \right]. \quad (4)$$

The component of multifractal decomposition  $\mathfrak{S}$  is

$$K_\alpha = \{x \in \mathfrak{S} \mid \lim_{n \rightarrow \infty} \frac{\log \mu(I_{i,n}(x))}{\log k_n} = \alpha\}. \quad (5)$$

It is more easy to analyze "coarse grained" Hölder exponents<sup>12</sup>  $\alpha = \alpha_n$  of  $\mu$  on  $I_{i,n}$ :

$$\alpha_n(I_{i,n}) = \frac{\log \mu(I_{i,n})}{\log k_n}. \quad (6)$$

Their variations are described by Legendre spectrum<sup>13</sup>:

$$f(\alpha) = f_L(\alpha) = \inf_q (\alpha q - \tau(q)), \quad (7)$$

where

$$\tau(q) = \lim_{n \rightarrow \infty} \frac{1}{\log k_n} \log \sum_i [\mu(I_{i,n})]^q \quad (8)$$

and summation runs through  $i$  such that  $\mu(I_{i,n}) \neq 0$ .

We analyze the radionuclide contamination data measured from the air for Karaganda and Semipalatinsk regions. The height of all flights was about 50 m and the velocity of the plane was about 125 km/h. Spectrometrical measurements were usually made at time intervals of 1 sec. The technique used is based on measurements of  $\gamma$ -quanta flow density of  $^{214}\text{Bi}$  (1.12 and 1.76 Mev) to determine the contamination by U,  $^{208}\text{Tl}$  (2.62 Mev) to determine *Th* contamination,  $^{40}\text{K}$  (1.46 Mev) to determine K and  $^{137}\text{Cs}$  (0.66 Mev) for *Cs* contamination. Total  $\gamma$ -activity is measured in the range of 0.25-3.0 Mev. The spectrometer was equipped by *NaI* element. The measurements have been done at different scales, e.g., in Karaganda and Semipalatinsk region the scale is 1:1,000,000, so the distance between paths is 10 kms. There are up to 11000 data points along the paths, with each reading separated by 50 meters. A sample of measured data can be found in Fig. 1.

For calculation of multifractal spectrum it is necessary to transform contamination values  $Y$  into probabilistic measures. As a rule, empirical probability density function  $p(Y)$  behaves itself as a curve (1) shown in Fig. 2, where function tails fall down. The path data  $Y$  were transformed to new variables  $Z$  which have rectangular random probability density function (the curve 2 in Fig. 2) by solution of

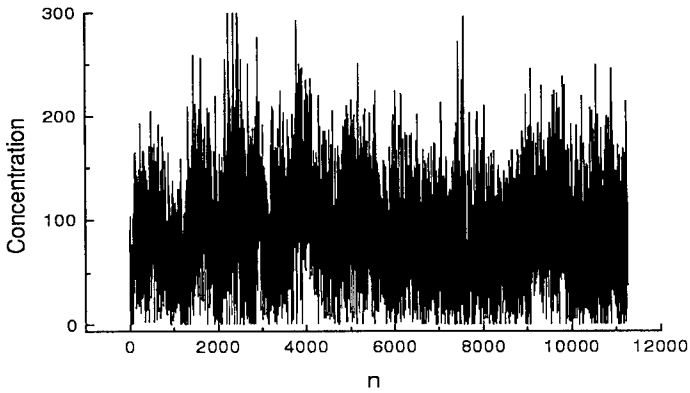


Figure 1. Data array of Cs, Semipalatinsk region path

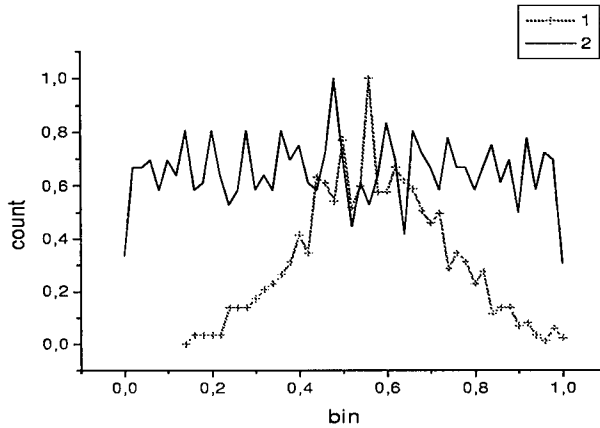


Figure 2. The histograms of distribution contamination data (1) and probabilistic measures (2).

equation  $P(Y) = P(Z)$ , where  $P$  is a probability function. In the case of rectangular random distribution  $Z = P(Y)$ . This transformation is equivalent to coordinate change which saves a dimension spectrum  $f(\alpha)$ <sup>14</sup>.

The range of  $q$  value was chosen as  $[-6, 4]$ . The Fig. 3 displays the set of multifractal spectra of radionuclide contamination of paths. The scaling of all isotopes obeys to multifractal law. The behaviors of  $f(\alpha)$  curves are different for various isotopes. In Fig. 4 it is shown the set of  $f(\alpha)$  spectra of man-made isotope Cs data calculated for different paths. It can be seen that scaling properties differ from path to path, but this scaling variability is not so high as distinction of  $f(\alpha)$

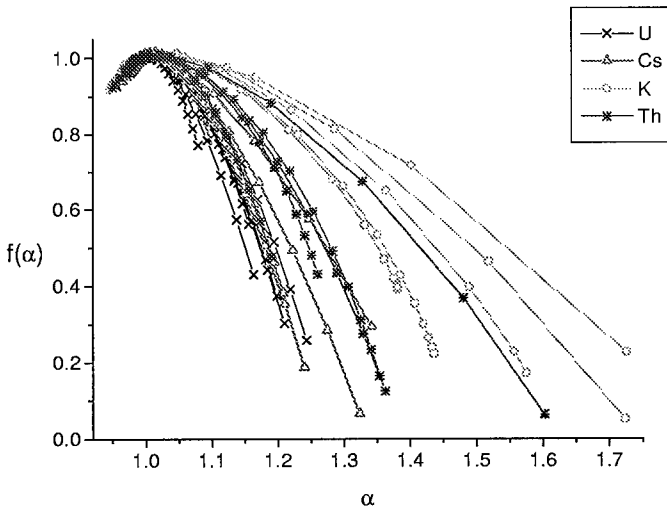


Figure 3. The set of  $f(\alpha)$  spectra of Karaganda path contamination.

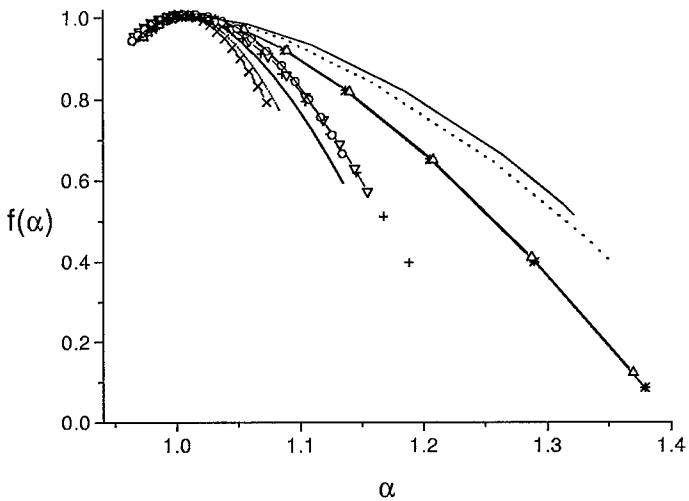


Figure 4. The set of  $f(\alpha)$  spectra of Cs data for some paths.

spectra for different isotopes (cf. Fig. 3).

The results obtained by multifractal tool are related to separate paths, where

a distance between adjacent paths is  $\sim 10km$  and effective strip of equipment capture is  $\sim 300m$ . For the case of measurements paving the territory we can use the method of computational topology described in the next section, which complements multifractal method.

### 3 Computational topology of the radionuclide fields: disconnectedness index.

The multifractal formalism can be applied to area contaminations, where a support of measure  $\mu(x, y)$  is a compact set  $X = [0, 1] \times [0, 1] \in \mathfrak{R}^2$ . In this case  $I_{i,n} \rightarrow I_{i,j,n}$ , where

$$I_{i,j,n} = \left[ \frac{i}{k_n}, \frac{i+1}{k_n} \right] \times \left[ \frac{j}{k_n}, \frac{j+1}{k_n} \right]. \quad (9)$$

Unfortunately, contamination data do not allow to use square paving, as the distance between the data points on adjacent paths is always larger than the distance between the neighbouring points along a single path. It could be used the tessellation of the surface by rectangles  $\{c_i\}$  <sup>15</sup>. In this case probability measure on  $c_i$  is averaged over rectangle, such as,  $\mu(x, y) : x, y \in c_i$  presents itself step-like function, which has a non-zero constant value at each rectangle. The components of "coarse-graining" multifractal decomposition  $K_\alpha$  are found by selecting of rectangles  $c_i$  of Hölder exponent  $\alpha \pm \Delta\alpha$ , where  $\Delta\alpha$  is discrete step of the measure. The coarse Hölder exponent is

$$\alpha(c_i) = \frac{\log \mu(c_i)}{\log |c|}, \quad (10)$$

where  $|c|$  is a size of  $c_i$ . "Coarse-graining" version  $f(\alpha)$  is

$$f_G(\alpha) = \lim_{\Delta\alpha \rightarrow 0} \lim_{\delta \rightarrow |c|} \frac{\log N_\delta(\alpha, \Delta\alpha)}{\log(1/\delta)}, \quad (11)$$

where  $N_\delta(\alpha, \Delta\alpha)$  denotes the number of boxes of  $\delta$  size with  $\alpha(c_i) \simeq \alpha$ . This function can be explained in statistical terms <sup>12</sup> as probability  $p_\delta$  of finding  $\alpha(c_i) \simeq \alpha$  and behaves roughly like

$$N_\delta(\alpha)/N_\delta = p_\delta [\alpha(c_i) \simeq \alpha] \simeq \delta^{D-f_G(\alpha)}. \quad (12)$$

Here,  $N_\delta$  is the total number of non-empty  $\delta$ -boxes which contain measure,  $D$  denotes the box dimension of the support of  $\mu$ .

For estimation of  $f_G(\alpha)$  spectrum it could be used functional box-counting <sup>15</sup>, however the covering by rectangle neighborhoods makes it impossible to re-scale rectangle edges uniformly and introduces additional local and global dimensions which have no clear meaning <sup>16</sup>. Consequently, we use computational topology for calculation of the box dimension  $f_G(\alpha)$ .

The component  $K_\alpha$  of multifractal decomposition is a subset  $\{c_i\}$  having the same  $\alpha \pm \Delta\alpha$ . The "coarse-graining" geometry of  $K_\alpha$  can be described by the rate of growth a number of  $c_i \in K_\alpha$  with improving resolution <sup>10</sup> and called *disconnectedness index*  $\gamma$ .

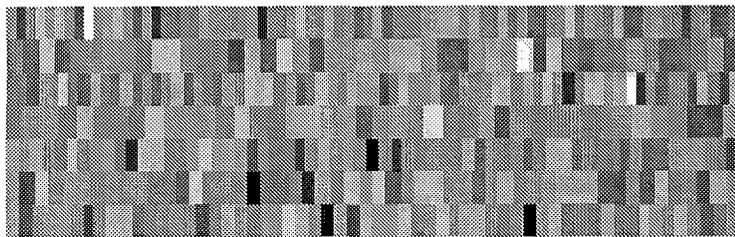


Figure 5. The paving map of U contamination of Irtys test site.

A topological space  $X$  is connected if and only if it cannot be decomposed into the union of two non-empty, disjoint, closed sets. If such a decomposition exists then  $X$  is said to be disconnected— that is, if there are two closed sets  $U$  and  $V$  such that  $U \cap V = \emptyset$  and  $U \cup V = X$ . There was reformulated the notion of connectedness in order to make it possible to implement a test for this property on a computer. The basic idea is to look at the set with a finite resolution  $\epsilon$  and see how connectedness changes as we let  $\epsilon \rightarrow 0$ . It is said that a subset  $X$  of metric space is  $\epsilon$ -disconnected if it can be decomposed into sets that separated by a distance of at least  $\epsilon$ .

Let  $N_\epsilon(\alpha)$  be the number  $\epsilon$ -components by given a resolution  $\epsilon$  and intensity of measure equals  $\alpha \pm \Delta\alpha$ . The disconnectedness index  $\gamma$  is the following limit:

$$\gamma = \liminf_{\epsilon \rightarrow 0} \frac{\log N_\epsilon(\alpha)}{\log(1/\epsilon)}. \quad (13)$$

The index equals to Hausdorff dimension for the simplest sets, for example for the middle-thirds Cantor set. However, more generally the disconnectedness index distinguishes between sets with the same box-counting dimension.

### 3.1 Scaling properties of Irtys area contamination.

There have been applied both multifractal formalism and computational topology to  $Th, K, U, Cs$  isotope contamination of Irtys area which is the part of STS. Irtys area was chosen for calibration of the devices for spectrometrical measurements from air and was investigated more thoroughly. The distance between paths was 50 m, effective strip of equipment capture was  $\sim 50m$  and there were 1197 measurements on the ground.

To calculate  $\gamma$  index a range of values for each isotope have been divided into 255 levels. The contamination values  $\nu(c_i)$  are expressed in the share of the whole range which was reduced to 1. In Fig. 5 a part of the digital image of contamination used for  $\gamma$  computation are shown.

The curves of disconnectedness index (Fig. 7) of natural isotopes have plateaux with  $\gamma = 2$  at  $\nu \in [0.3 \div 0.5]$  for  $Th$ ,  $\nu \in [0.3 \div 0.45]$  for  $K$  and  $\nu \in [0.3 \div 0.35]$  for  $U$  and the  $\gamma$  values decrease as  $\nu$  increases. The behavior of man-made  $Cs$  isotope is different. The index of disconnectedness  $\gamma$  is equal to 1.3 at a small  $\nu$  and slowly decreases demonstrating two plateaux:  $\gamma = 1$  at  $\nu \in [0.45 \div 0.7]$  and plateau  $\gamma \approx 0.6$  at  $\nu > 0.8$  (438 milliCurie/ $km^2$ ). The latter means the possibility of existence of

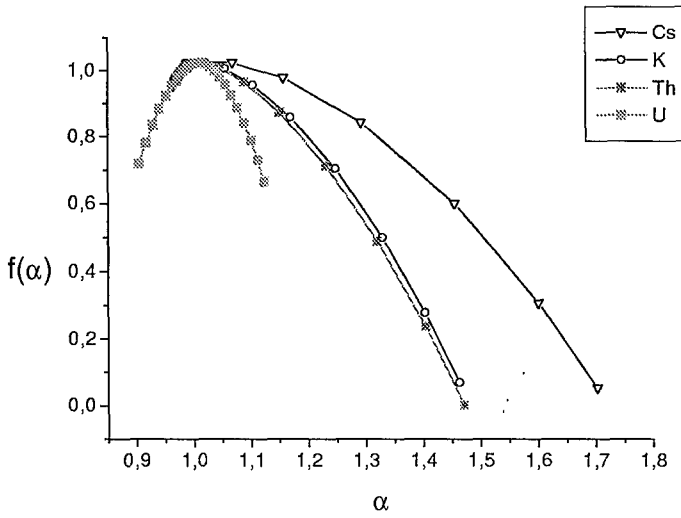


Figure 6. The  $f(\alpha)$  spectra of radionuclide data for Irtysch test site.

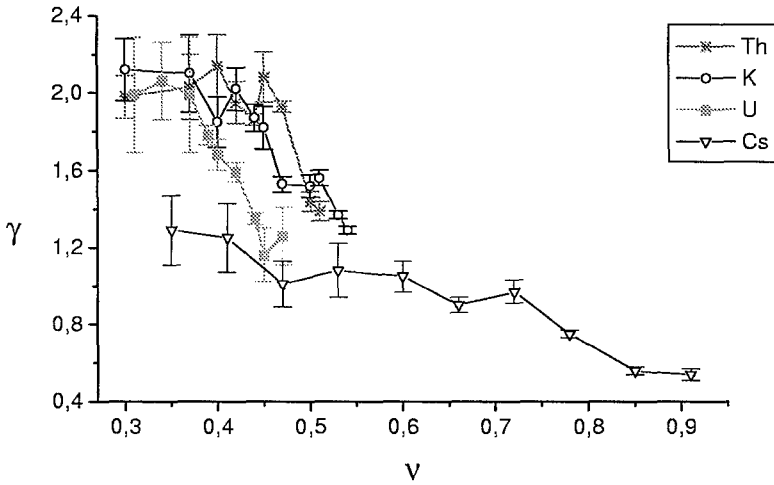


Figure 7. The dependence of disconnectedness index versus cross-section level for Th, K, U and Cs isotopes.

"hot spots" of  $Cs$  contamination which lie in the area of highest concentrations ( $> 438 \text{ milliCurie/km}^2$ ) and small fractal dimensions  $\gamma < 0.6$ . In general,  $\gamma(\nu)$  can be interpreted as "pre-multifractal" spectrum  $f_G(\alpha)$ . In this case, the probability of existence of "hot spots" decreases with spot size  $\delta$  as  $\propto \delta^{(2-\gamma)}$  (cf. Eq. 12). It is necessary to notice the similar behavior of  $Cs$  cumulative soil deposition data in Chechslovakia after Chernobyl accident<sup>6</sup>.

Statistical properties of multifractal fields are a function both of a scale and a dimension of a support of measurements. It is known, that measurement net with empirical box-dimension  $D_{net}$  cannot detect sparsely distributed phenomena with box-dimension  $D_a < 2 - D_{net}$ <sup>17</sup>. This conclusion follows from the common ideas about *transversality*<sup>18</sup>. It is necessary remember, that two sets  $M$  and  $N$  of dimension  $D_M$  and  $D_N$  intersect *transversally* in  $\mathfrak{R}^m$  if

$$\text{codim}(M \cap N) = \text{codim}D_M + \text{codim}D_N. \quad (14)$$

So, the net with dimension  $D_{net}$  can detect a set of dimension  $D_a$  only if  $D_{net} + D_a > m$ . As a rule, box-dimension of the net of spectrometrical measurements from air is  $D_{net} \ll 2$ , consequently, the number of anomalies on contaminated territories can be missed.

In addition to computation topology method there was used multifractal formalism for estimation of  $f(\alpha)$  spectra of Irtysh test site data. There was constructed one dimension array by linking all paths in one. Adjusted paths were "glued" together by taking into account their orientation and adding the beginning of the following path to the end of previous one. Such arrays were formed for all isotopes and multifractal spectra were computed. The results of this analysis are shown in Fig. 6. The comparison of results of both methods applied, to Irtysh data, points at good concurrence of isotope discrimination on their scaling. The qualitative behaviour  $f(\alpha)$  and  $\gamma(\nu)$  (Fig. 7) curves are the same. Man-made isotope  $Cs$  has demonstrated the most large Hölder exponent  $\alpha \sim 1.7$  in multifractal spectra. It means that there are hot spots of  $Cs$  contamination which form a sparse set having dimension  $f(\alpha) < 0.2$ .

#### 4 Conclusion

All the results of the multifractal analysis that we obtained support the existence of multifractal nature in the terrestrial radionuclides contamination in the two investigated regions and Irtysh area. The analysis made it possible to distinguish radionuclide isotopes  $K, Th, U, Cs$ , specially for measurements made on Irtysh test site.

Using the method of computation topology for the case of measurements paving the territory, a pre-multifractal spectrum of dimensions (indexes of disconnectedness) for Irtysh area was calculated. It was found that the behavior of disconnectedness index of natural isotopes differs strongly from  $Cs$  one. Contamination of natural radionuclides exhibits  $\gamma \approx 2$  for low values and dimension decreases quickly with increasing of level. Spectrum of dimensions for  $Cs$  points out the existence of "hot spots" of contamination.

Taking into account the multifractal properties of man-made  $Cs$  found for Irtysh

area, it can be pointed out the existence of dangerous for human health anomalies on all contaminated territories. These "hot spots" cannot be detected by using spectrometrical measurements from air accepted in Kazakhsatan. The results obtained can be the background of new methods of diagnostics of large territories.

### Acknowledgments

The support from INTAS-Kazakhstan grant number 95-0053 is gratefully acknowledged.

### References

1. Resolution of General Assembly of United Nations **A/Res/53/1D**, 7 (1998)
2. Yu.A. Izrael, Herald of the Russian Academy of Sciences **68**, 898 (1998) (in Russian)
3. G. Salvadori, S.P. Ratti and G. Belli, Health Physics **72**, 60 (1997).
4. M. Reginatto, P. Shebell and K.M. Miller, in *EML-590* ed. Environmental Measurements Laboratory, Department of Energy, U.S., October 1997
5. N. Makarenko, L. Karimova, and M.M. Novak, Fractals **6**, 359 (1998).
6. G. Salvadori, S.P. Ratti and G. Belli, Chemosphere **33**, 2359 (1996).
7. N. Makarenko, L. Karimova, and M.M. Novak, in *Proceedings of Fractals in Engineering* ed. (INRIA, 1999)
8. L. Barreira, Y. Pesin and J. Schmeling, Chaos **7**, 27 (1997)
9. K.J. Falconer, Jour. of Theoret. Prob **7**, 681 (1994)
10. V. Robins, J.D. Meiss and E. Bradley, Nonlinearity **11**, 913 (1998).
11. R.H. Riedi and J. Lévy Véhel, IEEE Transactions of Networking **3129**, 1 (1997)
12. R.H. Riedi and I. Scheuring, Fractals **5**, 153 (1997)
13. J. Lévy Véhel and J.-P. Berroir, Fractals in the Natural and Applied Sciences, IFTP **A-41**, 261 (1994)
14. M. Holschneider, Fractal Dimensions: A New Definition, M-CPT **2140**, 1 (1988)
15. S. Lovejoy and D. Schertzer and A.A Tsonis, Science **235**, 1036 (1987)
16. B.B. Mandelbrot, in *Fractals in Physics* ed. L. Pietronero and E. Tossati, North-Holland, Amsterdam, 1986
17. S. Lovejoy and D. Schertzer and P. Ladoy, Nature **319**, 43 (1986)
18. D. R. J. Chillingworth, in *Differential topology with a view to applications* ed. (Pitman Publishing London, San Francisco, Melbourne, 1976)